

# Functionalized Truxenes: Adsorption and Diffusion of Single Molecules on the KBr(001) Surface

Bartosz Such,<sup>†,‡</sup> Thomas Trevethan,<sup>‡,§,\*</sup> Thilo Glatzel,<sup>†</sup> Shigeki Kawai,<sup>†</sup> Lars Zimmerli,<sup>†</sup> Ernst Meyer,<sup>†</sup> Alexander L. Shluger,<sup>‡,||</sup> Catelijne H. M. Amijs,<sup>§</sup> Paula de Mendoza,<sup>§</sup> and Antonio M. Echavarren<sup>§</sup>

<sup>†</sup>Department of Physics, University of Basel, Klingelbergstrasse 82, 4056 Basel, Switzerland, <sup>‡</sup>Department of Physics and Astronomy, University College London, Gower Street, London WC1E 6BT, U.K., <sup>§</sup>Institute of Chemical Research of Catalonia (ICIQ), Av. Països Catalans 16, 43007 Tarragona, Spain, <sup>||</sup>Centre for Nanometer-Scale Science and Advanced Materials (NANOSAM), Jagiellonian University, Reymonta 4, 30-059 Krakow, Poland, and <sup>||</sup>WPI Advanced Institute for Materials Research, Tohoku University, Sendai 980-8577, Japan

The adsorption and diffusion of organic molecules on surfaces are integral to many areas of surface science and nanotechnology, such as self-assembly and growth of new surface structures, catalysis, coatings, corrosion inhibition, tribology, and molecular electronics. The advent of scanning probes, particularly the scanning tunneling microscope (STM), sparked an explosion of interest in studying the behavior and reactions of *individual* molecules at surfaces. This research was further stimulated by attempts to use individual molecules to perform computing functions.<sup>1–5</sup> Exciting new opportunities arose for imaging and manipulating individual molecules at conducting surfaces as well as creating prototype molecular devices<sup>6–10</sup> such as “wires”,<sup>11,12</sup> “switches”,<sup>13–16</sup> and molecular diodes, transistors, rectifiers, and small circuits.<sup>17–20</sup> Custom designed organic molecules are used as building blocks for the self-assembly of functional nanostructured materials.<sup>21–23</sup>

Different applications bring special requirements for molecular structure, properties, and mobility on the surface. For example, surfaces of insulators are often used as substrates for catalytic and photocatalytic reactions. Reliable functioning of a molecular electronic device requires that the molecule has to be immobilized and stable at room temperature (RT), but the electronic structure of the molecule must be decoupled from that of the surface. However, when organic molecules are adsorbed on a metallic substrate, the molecule–surface interaction may induce changes in the molecular structure and properties as well as local modifications in the surface geomet-

**ABSTRACT** In this work, we have studied the adsorption and diffusion of large functionalized organic molecules on an insulating ionic surface at room temperature using a noncontact atomic force microscope (NC-AFM) and theoretical modeling. Custom designed *syn*-5,10,15-tris(4-cyanophenylmethyl)truxene molecules are adsorbed onto the nanoscale structured KBr(001) surface at low coverages and imaged with atomic and molecular resolution with the NC-AFM. The molecules are observed rapidly diffusing along the perfect monolayer step edges and immobilized at monolayer kink sites. Extensive atomistic simulations elucidate the mechanisms of adsorption and diffusion of the molecule on the different surface features. The results of this study suggest methods of controlling the diffusion of adsorbates on insulating and nanostructured surfaces.

**KEYWORDS:** KBr · atomic force microscopy · diffusion · molecular dynamics · truxenes

ric and electronic structure. Due to these reasons, wide gap insulators are more appropriate substrates for designing reliable molecular devices. However, very little is still known about the adsorption and diffusion of organic molecules on wide gap bulk insulating surfaces or films. Therefore, no method has been suggested so far for tailoring the molecule–substrate interactions to control the molecular diffusion while producing films or molecular devices with desired morphologies, and trials have been mainly empirical. The purpose of this work was, therefore, to test design criteria for adsorbing organic molecules with given properties at inert insulating surfaces and to study their diffusion using atomic force microscopy at RT. In the course of this study, we were able for the first time to directly observe the diffusion of a complex organic molecule on an insulating surface.

To conceive, synthesize, deposit, and image single molecules on a wide band gap insulating surface at RT is a complex task, which so far has not been achieved. In contrast to metallic surfaces, where aromatic

\*Address correspondence to t.trevethan@ucl.ac.uk.

Received for review March 2, 2010 and accepted May 07, 2010.

Published online May 25, 2010. 10.1021/nn100424g

© 2010 American Chemical Society

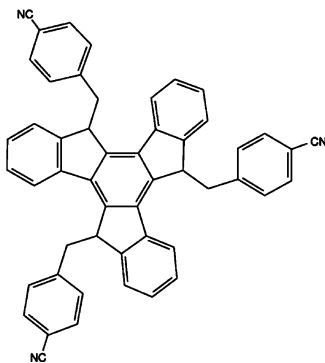


**Figure 1.** Chemical structure of the molecule employed in this study: *syn*-5,10,15-tris(4-cyanophenylmethyl)truxene.<sup>44</sup>

boards provide sufficient anchoring,<sup>24</sup> insulating surfaces exhibit much weaker interactions with these molecules. To be immobilized on an ionic crystal surface, a hydrocarbon molecule has to be functionalized with special anchoring groups. Moieties possessing a large dipole moment were shown to adsorb quite effectively (*e.g.*, cyanoporphyrins),<sup>25,26</sup> albeit the molecular agglomerates were additionally strengthened by molecular  $\pi-\pi$  stacking. The adsorption of the C<sub>52</sub>H<sub>72</sub>O<sub>3</sub> molecule, consisting of three 3,5-isobutyl phenyl headgroups (derivatives of *m*-xylene) and an ethyl formate tail group, on the rutile TiO<sub>2</sub>(011) surface, has recently been studied theoretically in ref 27. The adsorption and diffusion of anthracene and tetracene molecules on the rutile surface have been modeled in ref 28. The molecules considered in refs 27 and 28 were all functionalized by polar carboxylic groups, which provided attachment to the surface.

To study individual molecules on insulating surfaces in UHV, it is necessary to use a noncontact atomic force microscope (NC-AFM), which relies on detecting tip–surface forces. AFMs capable of atomic resolution are challenging to construct and operate (see, for example, refs 31–33). On the other hand, weak adsorption and high mobility of organic molecules at insulating surfaces often prevent AFM imaging of individual molecules at RT. The best studied is perhaps adsorption of perylene and its derivatives (*e.g.*, PTCDA and PTCDI) which have been imaged on several insulating substrates, such as KBr, KCl, NaCl, mica, and TiO<sub>2</sub>(110);<sup>34–40</sup> however, in all of these studies, large assemblies of molecules were imaged, and the successful imaging of isolated molecules remains rare.

The molecule conceived for this study is *syn*-5,10,15-tris(4-cyanophenylmethyl)truxene, which contains three flexible cyanobenzyl groups, each possessing a large dipole moment, as shown in Figure 1. This molecule belongs to a class of organic molecules that are relevant to molecular devices—a flat polycyclic core bonded to several (in this case three) flexible “binding groups” that interact strongly with the surface. The KBr surface is employed due to it being a very stable wide band gap insulator. This surface is easy to prepare and

modify, and it has been successfully imaged many times previously with the NC-AFM.<sup>29,30</sup> On the basis of previous studies, we assumed that these molecules can be deposited at the KBr surface; however, there was no guarantee that we could observe and study individual molecules. As we show below, in spite of the strong adsorption, the truxene molecule is indeed surprisingly mobile both on the terrace and at a step edge of KBr.

The STM and NC-AFM can be useful in providing “snap shots” of the overall dynamics of an adsorbate and can be used to determine overall hopping rates and diffusion coefficients, but they are not capable of probing the fundamental atomic scale mechanisms of adsorbate motion, which can occur over time scales from seconds to picoseconds. The only way to gain an insight into the actual processes that drive the overall behavior is through realistic atomistic simulations. The use of simulations has helped to understand the mechanisms of surface diffusion in many systems, from single adatoms on a perfect surface to the collective motion of atomic clusters and large organic molecules on defective and low symmetry surface features. The most direct way of investigating the thermal diffusion of adsorbates is with an equilibrium molecular dynamics (MD) simulation, where the trajectory of the phase-space atomic coordinates of the system (which includes both adsorbates and the surface) is followed explicitly and in real time. MD has been used to explain the specific mechanisms of surface diffusion in many systems including the “long jumps” of adatoms observed in STM experiments<sup>41</sup> and of large organic molecules on a variety of surfaces<sup>42,43</sup> and how these systems depart from the transition state theory model. In this paper, we use MD to develop a comprehensive theoretical model of the adsorption and diffusion of a truxene molecule on the KBr(001) surface.

## RESULTS AND DISCUSSION

The simulations performed in refs 27 and 28 have demonstrated that the overall structure and flexibility of an organic molecule has a profound effect on the mechanism of diffusion and the effective diffusion rate on a surface. Very small structural changes may cause differences in their mobility on the surface by many orders of magnitude. The potential energy landscape of the molecule/surface system is determined not only by the chemical interaction between the surface and the binding groups but also by the structure of the entire molecule relative to the surface. Bearing this in mind, we decided to study a molecule derived from heptacyclic polyarene truxene (10,15-dihydro-5H-diindeno[1,2-*a*;1',2'-*c*]fluorene), where three 4-cyanobenzyl groups have been added in positions 5, 10, and 15 in a *syn* relative configuration (see Figure 1). The synthesis and characterization of this class of molecules has been described in ref 44. As a result, this tris(4-cyanophenylmethyl)truxene (PM\_4CN) molecule pos-

sesses three strong dipole groups (the dipole moment for the benzonitrile molecule was calculated to be 4.5152 D<sup>45</sup>), which are capable of adjusting their positions in order to match the electrostatic landscape on the substrate. The aromatic component of the molecule is separated from the surface by the binding groups and therefore interacts only weakly with the surface.<sup>27</sup> The long binding groups are free to move somewhat independently on the surface, and this flexibility allows the binding groups to easily bind to separate binding sites, which may increase the binding to the surface.

The KBr(001) surface was prepared by cleaving and then annealing in vacuum. The surface was then irradiated with a small dose of 1 keV electrons, which led to desorption of less than 0.5 ML of KBr. The electron-induced desorption results in the creation of monolayer pits of different sizes dependent on the electron dose.<sup>29,30</sup> In the areas of high density of cleavage steps, desorption proceeds from existing steps leading to their erosion.

The truxene molecules were then deposited on the surface *via* evaporation from an effusion cell (resulting in a coverage of approximately 40% of a monolayer, as determined from several large-scale NC-AFM images) and then imaged using the NC-AFM.<sup>46</sup> The NC-AFM is based on monitoring and controlling the resonance frequency of a small oscillating cantilever with a tip attached at its end while it is moved across the surface. The interactions (chemical, van der Waals, electrostatic) between the tip and the sample change the cantilever resonance frequency, allowing for the determination of their spatial variation down to the atomic scale.<sup>31,32,47</sup>

Figures 2 and 3 show NC-AFM images of the KBr surface with the molecules adsorbed. Immobilized molecules are imaged as bright protrusions and are located adjacent to the terrace edges of KBr. Figure 2a shows a large surface area revealing several terraces and islands, and Figure 2b,c shows magnified sections centered over a kinked monolayer step edge. No molecules are observed on the perfect (001) terrace at any point. We observed obvious differences in the monolayer step edge decoration: those running in the main crystallographic directions [100] and [010] are not decorated by stable molecules in contrast to the edges deviating from those directions. The analysis of the KBr atomic resolution pattern (Figure 2c) reveals that the edge is running in the [-310] direction, which is the most common direction found for regularly decorated edges on that surface.

The molecules adsorbed on the edge presented in Figure 2c are spaced by approximately 2.1 nm. The step edges of KBr are electrically neutral; therefore, the [100] and [010] directions are preferred. In order to align directions such as [-310], the edges most likely adopt jagged conformations such as that shown in Figure 2d. Note that the distance between the neighboring kinks for the [-310] jagged edge is very close to the intermo-

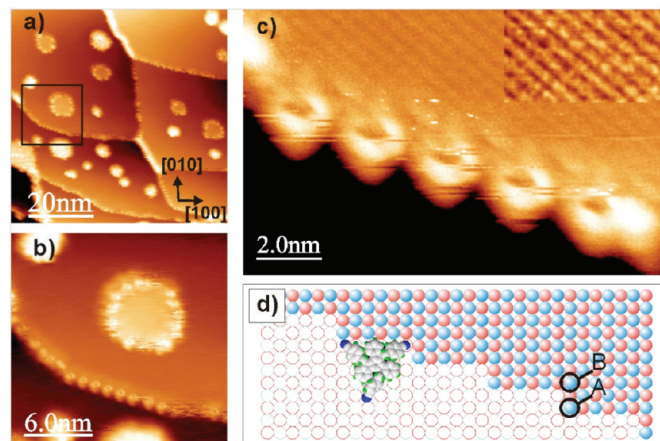


**Figure 2.** NC-AFM images of truxene molecules adsorbed on the patterned KBr(001) surface: (a)  $65 \times 65 \text{ nm}^2$  image showing several islands and terraces (normalized frequency shift<sup>32</sup>  $\gamma = -0.97 \text{ fNm}^{1/2}$ ); (b) magnified view of the section highlighted in (a); (c)  $10 \times 6.3 \text{ nm}^2$  image showing details of a monolayer KBr step decorated by the molecules; the inset shows the atomic periodicity with enhanced contrast. (d) Proposed configuration of the step imaged in (c) and a possible position of a molecule. Positions A and B are discussed in the text.

lecular distance of 2.1 nm. There are two characteristic points in the jagged edges: the outermost ion (marked A in Figure 2d) and the innermost ion (marked B). In all of the observed edges, the ions in position A are of the same sign (negative in Figure 2d) and the ions in position B are of the same sign (in the example from Figure 2d, also negative).

It is impossible to rule out some molecule–molecule interaction between the molecules adsorbed at the jagged edges, although it is unnecessary for the immobilization of the molecules since their stabilization at the kinks is the result of molecule–substrate interaction only. There are edges on the surface running straight in [100] or [010] directions for several nanometers with only a small number of separated kinks. An example of such a case is presented in Figure 3, where a single kink is located in the middle of the figure. This kink is sufficient to immobilize a single isolated truxene molecule.

In addition to a stable molecule located at the kink site in Figure 3, a noisy pattern along the [010] step

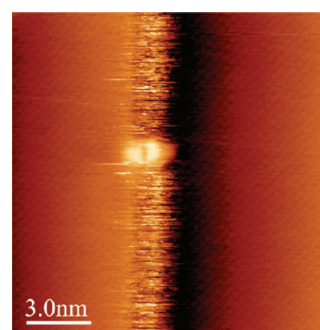


**Figure 3.** A  $15 \times 15 \text{ nm}^2$  NC-AFM image ( $\gamma = -0.70 \text{ fNm}^{1/2}$ ) presenting a KBr edge with a single kink and a truxene molecule immobilized. The noisy pattern along the [010] monolayer step edge is due to rapidly diffusing molecules.

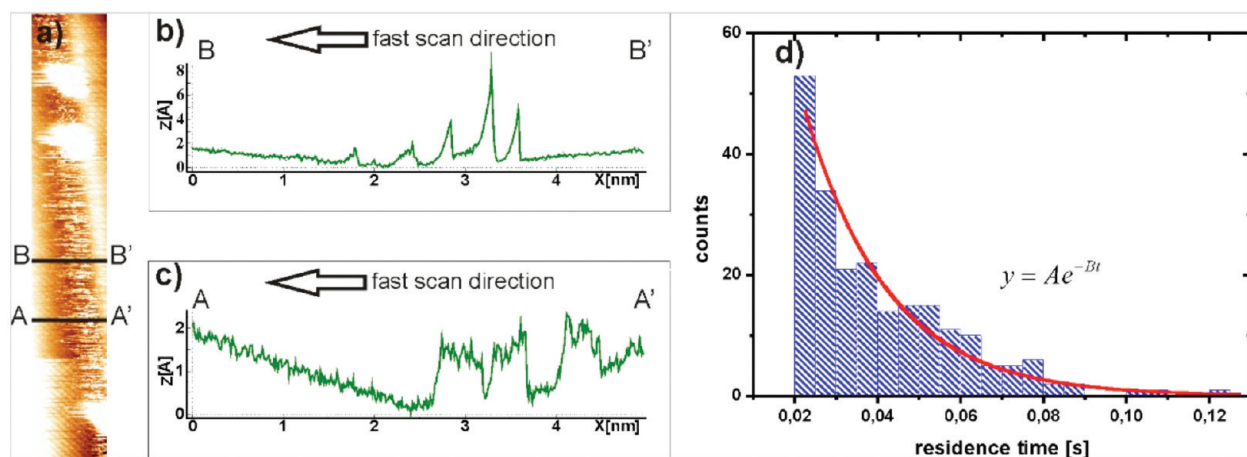


**Figure 4.** (a) A  $5 \times 30 \text{ nm}^2$  image ( $\gamma = -0.59 \text{ fNm}^{1/2}$ ) of a step edge with three molecules immobilized and noisy pattern between. (b) Cross section along the B–B' line in (a), showing asymmetric features; in individual scan lines taken in the opposite directions, the shape of instabilities is mirrored. (c) Cross section along the line A–A', showing the symmetrical instabilities with the shape independent of the scan direction. (d) Histogram showing distribution of lengths of symmetric features; the exponent is fitted with  $B = 50 \text{ s}^{-1}$ .

edge can be seen. This pattern is formed by “stripes” caused by rapid variations in contrast within a single scanline; that is, the contrast is changed as the tip scans along the step edge (the fast scan direction is from left to right). This occurs stochastically and is not directly related to the tip position above the surface, resulting in a somewhat random or fuzzy pattern, which consists of a collection of lines with a non-uniform distribution of lengths. This feature can be attributed to changes in the surface structure as the oscillating tip is scanned above the surface (for a detailed description of this phenomenon, see ref 48 and 49). The most plausible explanation for this structural change is the diffusion of truxene molecules along the step edge, which is occurring much faster than the time required to acquire a single image. The forms of the lines consist of two typical shapes, as depicted in Figure 4b,c. The first of these features (Figure 4b) is asymmetric, and the shape is dependent on the tip scanning direction. The feature is characterized by an abrupt lift of the tip with a considerably slower recovery to the previous position. The feature is often observed in series. That shows that a molecule suddenly appears in the area under the tip and stays there long enough to allow the tip to move over. The dependence of the shape of the feature on the scanning direction points to a tip-induced process, and a molecule is most likely immobilized and/or pulled by the tip apex. This results in a tip-induced manipulation (or similarly “stimulated diffusion”).

The second feature (Figure 4c) has a symmetrical and rectangular shape, which is independent of the scanning direction of the tip. Here, the length of this rectangular feature represents the residence time of a molecule in a particular adsorbed state due to the fact that the tip scans the surface at a constant velocity. Since the scanning speed in the fast direction in Figure 4a was  $10 \text{ nm/s}$ ,  $1 \text{ nm}$  in this image corresponds to a time of  $0.1 \text{ s}$ . By measuring the length of each of the

rectangular shaped lines that correspond to spontaneous transitions, it is possible to plot a distribution of residence times that is shown in Figure 4d. This distribution follows an exponential form, which corresponds to an average residence time of approximately  $200 \text{ ms}$ .

The results detailed above show three distinct features with respect to the mobility of the molecules on the surface. First, individual molecules are observed as stationary at monolayer kinks and along the  $(-310)$  monolayer (kinked) step edge; this demonstrates that the average residence time for the molecules adsorbed on these features is significantly longer than the time taken to acquire several successive images, which corresponds to over an hour. Second, the “fuzzy” pattern observed along the  $(010)$  monolayer step edge shows that adsorbates are diffusing significantly faster than the time required to acquire a full image but slower than the time taken to resolve changes along a particular scan line, resulting in the stripes that form the fuzzy pattern. Third, no molecules are observed on the perfect terrace, but the surface atoms are resolved. This shows that either the molecules do not adsorb on the terrace at all or they are diffusing at a rate significantly faster than the time required to resolve changes in height as the surface is scanned, or they diffuse quickly to step edges and other defects even before the NC-AFM imaging starts.

To understand the features observed in the NC-AFM images described above and to determine the mechanisms of the adsorption and mobility of the truxene molecules on the KBr surface, atomistic simulations to model this system were performed. This modeling consisted of a combination of accurate quantum chemical calculations to determine the nature of the interaction of the molecules with the surface and extensive MD simulations of the diffusion mechanisms employing a parametrized potential model.

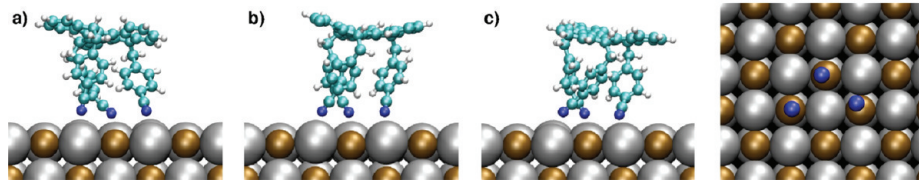


**Figure 5.** (a) Lowest energy configuration of the molecule adsorbed on the KBr terrace, obtained from simulated annealing. (b,c) Two alternative configurations with adsorption energies of (b) 0.59 and (c) 0.60 eV. (d) Lateral positions of the N atoms in the three binding groups above the K atoms in the surface for the lowest energy configuration.

**Ab Initio Calculations.** To characterize the chemical interaction of a truxene molecule with the KBr surface, the interaction of the basic hydrocarbon molecular groups, methane and benzene, and benzonitrile group which constitute the molecule with the surface was investigated using an embedded cluster quantum chemical method<sup>50,51</sup> employing the B3LYP hybrid functional,<sup>54,55</sup> which is well-suited to reproduce the electronic structure of both the molecule and the KBr surface.

For each of these molecules adsorbed in various orientations on the terrace and step and corner edges, it was found that there is no chemical interaction with the surface: no significant charge transfer occurs ( $<0.02$  e), and it is energetically unfavorable for the molecules to deprotonate on the surface or step. The hydrocarbon molecules interact with the surface relatively weakly, with the benzene having a maximum adsorption energy of 0.08 eV (0.02 eV) and methane of 0.03 eV (0.01 eV) on the perfect terrace (counterpoise corrected energies are given in brackets<sup>53</sup>).

The interaction of the truxene molecule with the surface is dominated by polar CN groups of the benzonitrile molecule since they adsorb above K ion sites in the perfect surface with an energy of 0.23 eV (0.19 eV). The electronic structure of each of these molecules is negligibly polarized by the interaction with the surface, and the mechanism of binding in each case is ionic.

The B3LYP functional is known to significantly underestimate the magnitude of the van der Waals interaction. To investigate the magnitude of this discrepancy, we performed a limited number of calculations employing the MP2 method,<sup>56</sup> which includes some correlation effects. Using this method, the maximum adsorption energy of benzene increases to 0.20 eV, although this is reduced to 0.08 eV when counterpoise corrected (the same as the non-counterpoise-corrected B3LYP energy). The maximum adsorption energy of cyanobenzene increases to 0.28 eV, which is reduced to 0.21 eV when counterpoise corrected (similar to the 0.23 eV non-counterpoise-corrected B3LYP energy). Therefore, the effect of the van der Waals interaction is expected to be relatively small in this system, and non-additive effects are also expected to be small as the binding groups are not fully conjugated with the truxene core.

**Modeling Truxenes on KBr(001).** Modeling the adsorption and dynamics of the entire molecule on the surface is not computationally feasible using an *ab initio*

method directly due to the system size. Therefore, interatomic pair potentials were derived for the interaction of each of the functional groups with the surface and combined following the methodology outlined and tested in refs 27 and 57. In this system, this approach is accurate because the interaction of the molecule with the surface can be described with an ionic model as no charge transfer between the molecule and surface takes place. This potential model allows extensive investigation of adsorption conformations and molecular mobility with relatively low computational cost.

Employing the potential model described above, we investigated the adsorption of the truxene molecule on the KBr(001) terrace. To determine the lowest energy adsorbed conformations of the truxene molecule, the system is annealed using MD annealing<sup>63</sup> from various initial conformations, with the molecule in different lateral positions and orientations above the surface. The MD annealing is run at temperatures of up to 500 K (which is sufficient for the molecule to access all structural states) for up to 1000 ps, and then slowly cooled to 0 K over a period of 500 ps. The lowest energy conformation of the molecule on the terrace shown in Figure 5a is characterized by the CN groups binding to three adjacent K sites on the surface and the flat polyaromatic truxene core of the molecule approximately parallel to the surface plane. The binding energy of this configuration (*i.e.*, the potential energy difference between this state and the relaxed molecule and surface separated to infinity) is 0.60 eV. For this configuration of binding groups on the surface, there are several different conformations of the truxene skeleton, which are very similar in energy to the ground state, based on the relative orientations of the benzonitrile rings of the flexible cyanobenzene groups, which arrange themselves to bind to the surface K sites. Examples of two such conformations are shown in Figure 5b,c. Due to the complexity of the molecular structure and the large number of possible conformations of the molecule on the surface, the absolute binding energy in the static minimum energy conformation of the system is only of limited interest since the system will spend little time in this state. A better measure for comparison of the overall binding to the surface at a particular temperature is the difference in average total energies between the bound and unbound (desorbed) states. This “average” binding energy will then contain contributions from all of the different states sampled as

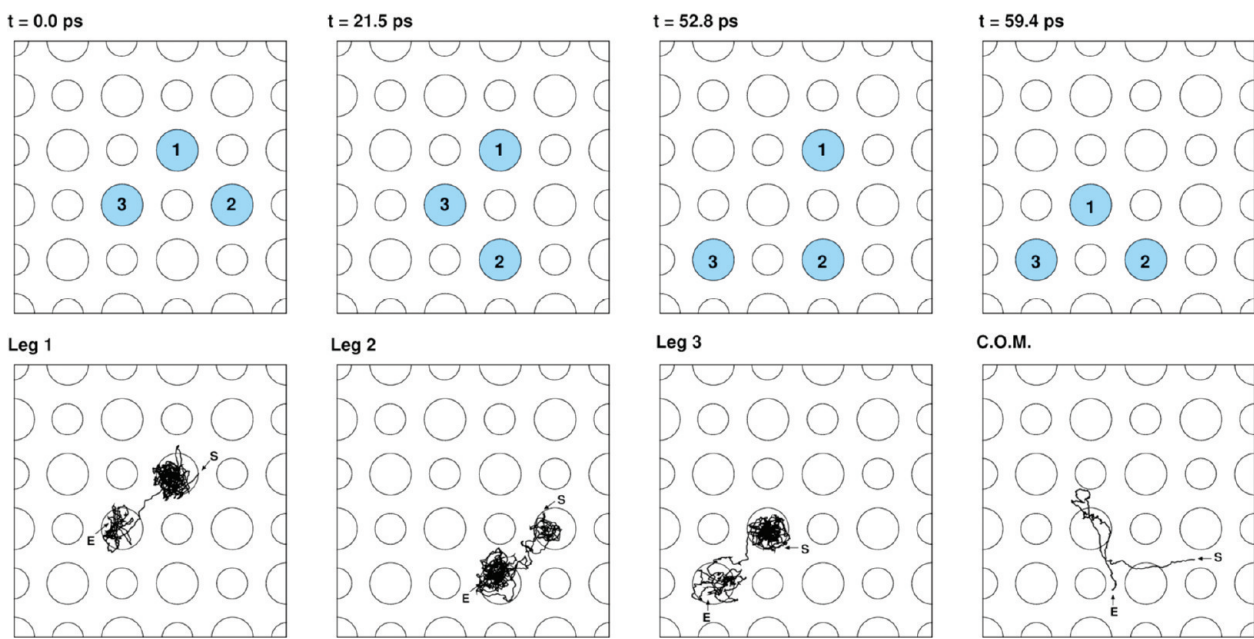


**Figure 6.** Top panels: sequence of the positions of the binding groups on the KBr surface during a single translational transition between equivalent ground states (large circles denote K ion positions). Bottom panels: lateral trajectories of the N atoms in the three binding groups of the molecule (labeled above) and of the center of mass of the rigid board of the molecule over the entire transition. The start and end points of the transition are labeled.

the molecule moves on the surface. To calculate this difference, the average total energy of the bound system, the isolated molecule, and the isolated surface is determined over a long (10 ns) MD simulation at 300 K. The average binding energy is then calculated to be 0.42 eV, which is approximately 0.2 eV lower than the static binding energy, which suggests that the adsorbed molecule is spending a significant proportion of time in states substantially higher in energy than the global minimum.

**Surface Diffusion.** Room temperature MD calculations show that the skeleton of the molecule and the orientation of the benzonitrile groups undergo rapid transitions between different states of similar energy on the time scale of picoseconds, while transitions of the binding groups between sites happen much more rarely. The movie included in Supporting Information shows a side view the evolution of structure of the molecule over a period of 500 ps. The molecule remains with all three binding groups bound to specific K atoms in the surface for a significant period of time relative to the motion between similar energy states of the skeleton of the molecule, due to the relatively strong binding of the CN groups to the K atoms in the surface.

The molecule diffuses on the surface *via* hops of the benzonitrile binding groups to nearest neighbor K binding sites, and also longer hops to non-nearest neighbor K sites as individual binding groups are temporarily desorbed from the surface. The movement of the molecule as a whole is a product of the collective motion of all three binding groups and therefore occurs significantly more slowly than the diffusion of a single group (a single cyanobenzene molecule). It is significant

to note that a single cyanobenzene molecule will desorb from the surface at room temperature (determined from MD calculations) with an average residence time of  $\sim 250$  ps. A movie of the top view diffusion of the molecule over a time period of 1 ns is shown in Supporting Information, which also shows the evolution of the positions of the binding sites. Extensive molecular dynamics calculations over much longer time scales show that the molecule is bound to, but highly mobile on, the surface at RT, with a surface diffusion coefficient of approximately  $10^{-7} \text{ cm}^2 \text{ s}^{-1}$ , which corresponds to a root-mean-square displacement of approximately 1  $\mu\text{m}$  after a period of 3  $\mu\text{s}$ .

In order to consider the mechanism of diffusion of the molecule on the surface in more detail, we define a “ground state” of the molecule as a configuration in which all three binding groups are bound to three adjacent K surface ions, in a triangular formation, as shown in Figure 6. This state corresponds to the lowest energy states of the system. To enable the diffusion of the molecule, one binding group will leave the ground state, either through desorption or a hop to a nearest neighbor K site. If desorption of a group occurs, it may either readsorb on the same site or a nearby (not necessarily a neighboring) K ion site. A particular ground state where all CN groups are bound to surface K ions is occupied for the majority of the time; the remainder of the time the molecule is in an intermediate state that will either return to the initial ground state or allow the molecule to move into an adjacent ground state where the molecule will have diffused one lattice distance in a particular direction. A typical sequence of these transitions between ground states in terms of the

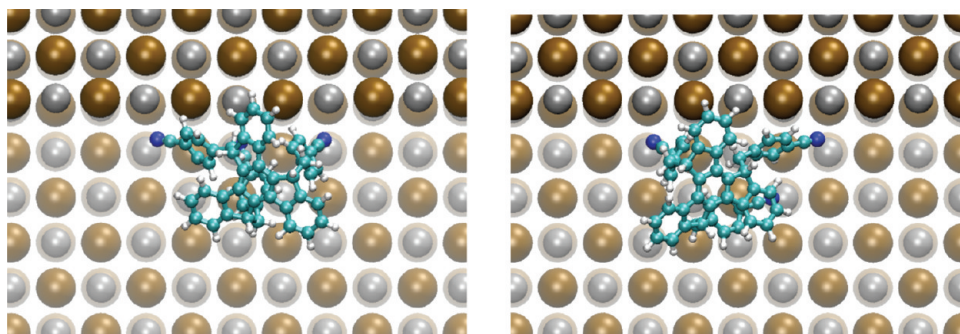


**Figure 7.** Left: Configuration of the molecule bound to the step edge (K ions are light gray) in its lowest energy state (determined from simulated annealing). Right: Configuration with one binding group moved away from the step edge and bound to a K atom one lattice distance away on the terrace.

positions of the binding groups is shown in Figure 6, along with the times the different transitions occur. For this particular transition, the lateral trajectory of the N atoms of each of the binding groups and the center of mass of the truxene core of the molecule is also shown. Here, it can be seen how the  $-CN$  groups oscillate in the deep potential basins due to the strong binding between the groups and K ions before undergoing transitions to nearest neighbor positions. The transition of a single binding group from one K site to another occurs when that part of the molecule is sufficiently excited, either by surface vibrational modes or by modes from the truxene skeleton of the molecule. However, the separation of the individual  $-CN$  groups through the molecular structure spatially results in very little vibrational correlation between different binding groups.

**Modeling Truxenes at the [010] Monolayer Step Edge.** It is useful to characterize the interaction of the molecule with the step edge by calculating the adsorption binding energies of a single cyanobenzyl binding group molecule at the step. The polar CN group interacts more strongly with the monolayer step edge than with the terrace: a deep potential well created by two adjacent K ions in the step acts to bind the molecule with an energy of 0.49 eV. Adsorbing the entire truxene molecule on the step edge, the molecule can access several conformations that are characterized by the relative positions of the cyano binding groups on the double coordinated K sites along the step edge. The lowest energy of these is with each of the cyano groups binding to three adjacent sites coordinated by two K ions along the step, as shown in Figure 7a. This configuration has a static binding energy of 1.01 eV (determined using the same simulated annealing procedure described above). The next significantly lower energy conformation shown in Figure 7b corresponds to a binding energy of 0.87 eV and is characterized by one of the three binding groups away from the double coordinated step sites and bound to a terrace K atom one interatomic distance away from the step edge.

MD simulations of this system in the ground state conformation show that the truxene skeleton is more confined than when on the terrace. In this case, the ori-

entations of the benzyl substituents of the binding groups also fluctuate much less than at the terrace, resulting in a significant reduction in the entropy in this state compared to the molecule on the terrace. A movie of the structure of the molecule over a time period of 5 ns is included in Supporting Information. The average binding energy of the truxene molecule adsorbed at the step edge at room temperature is again determined as above and is 0.78 eV, which is approximately 0.25 eV lower than the static binding energy in the global minima. Again, this is indicative of the system spending significant periods of time in higher energy states (e.g., with one of the binding groups away from the step edge).

Over long time scales of the MD simulation, the truxene molecule demonstrates several very rare jumps between adjacent ground state conformations over the entire simulation run of 100 ns. This does not allow for an accurate determination of the rate of diffusion but puts an upper limit on the residence time of the molecule in a minimum energy state of approximately 10–30 ns.

The mechanism of the diffusion of the molecule along the step edge consists of individual binding groups moving out of the deep potential well caused by the double coordinated K sites at the step edge, to a terrace K site (as shown in the conformations in Figure 7b). In order for the molecule to move one lattice distance along the step edge into a neighboring ground state, at least two of the binding groups must leave their step-K sites and move to new positions, at the same time, due to the constraints of the molecular structure. This results in a structural transition along the step being extremely rare (relative to individual binding groups leaving the step edge minima). This is due to the fact that, when a binding group leaves a step-K site, the probability for it to then return is much higher than the probability of a second binding group leaving its step-K site. A typical sequence of binding group positions of the molecule along the step edge during a single successful molecular transition is shown in Figure 8. Note that, in the majority of cases when the sys-

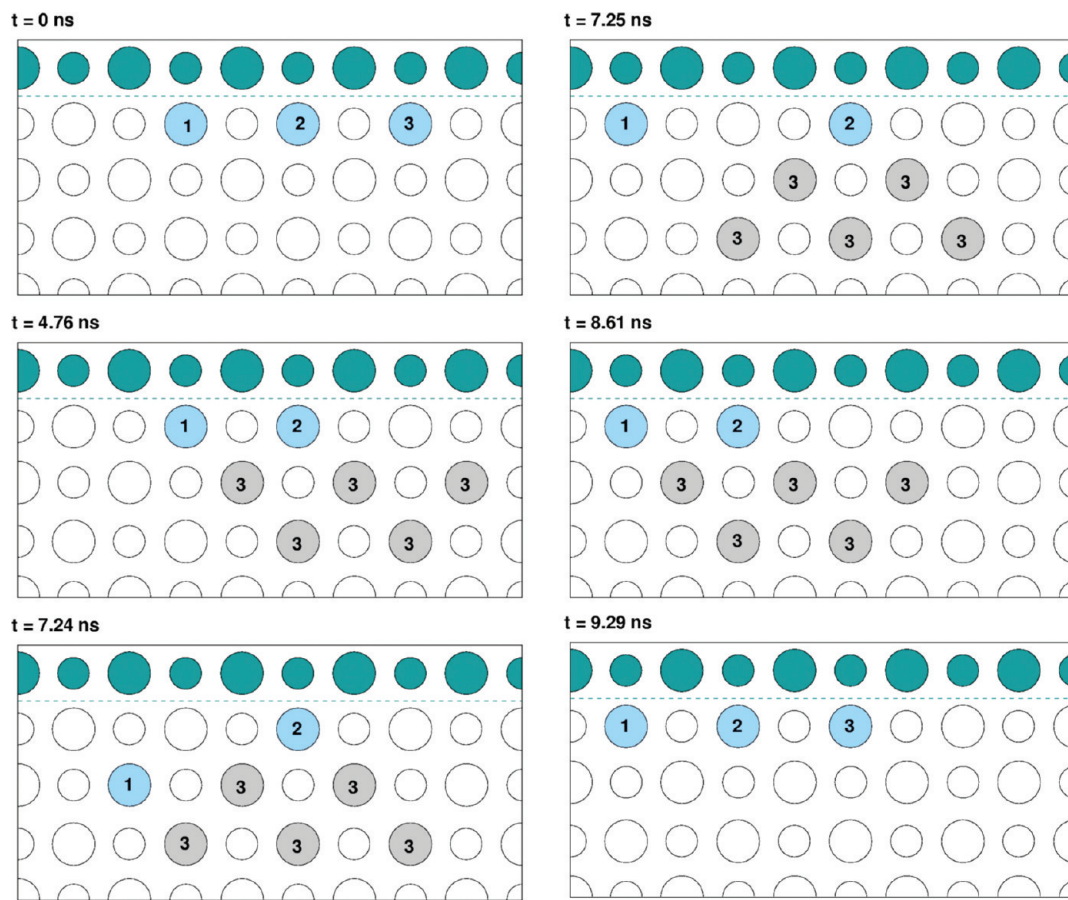


**Figure 8.** Sequence of binding group positions for the molecule moving one lattice distance along the monolayer step edge, along with the transition times. When a particular leg moves away from an edge position, it can move quickly into a new edge position or move rapidly between surface K sites away from the step edge for some period of time, as shown here for leg 3.

tem leaves a ground state, it will eventually return without a change in the position of the molecule.

It is also significant to note that MD calculations show that a single benzonitrile molecule diffuses away from the step edge at room temperature (with an average residence time of approximately 3 ns) and then desorbs from the terrace. This shows that it is the collective and combined motion of all three binding groups that is required to confine the molecule to the step edge, even though they are able to move somewhat independently.

**Modeling Truxenes at Monolayer Kinks.** The benzonitrile molecule interacts differently with the two different polarity double atomic kinks; for the K terminated kink, the molecule binds to the terminating ion with an energy of 0.46 eV. For the Br terminated kink, a deep potential well created by three adjacent K ions in the corner position binds the molecule with an energy of 0.61 eV. The lowest energy structure of the truxene molecule adsorbed on the K terminated double atomic kink shown in Figure 9b corresponds to a binding energy of 1.17 eV. This structure is characterized by one CN

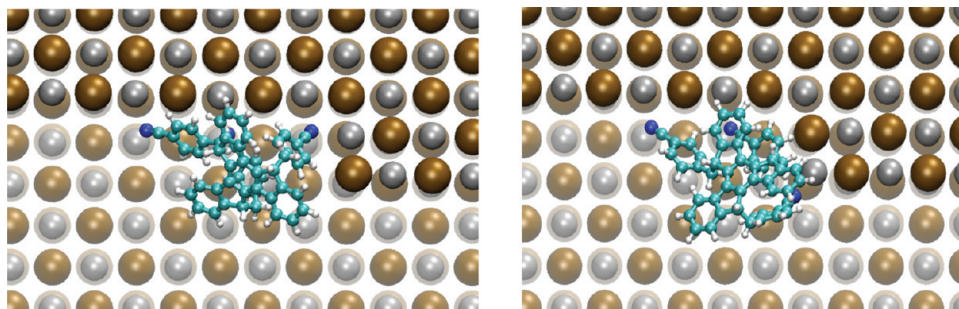


**Figure 9.** Left: minimum energy configuration of the molecule adsorbed on the Br terminated double layer kink. Right: minimum energy configuration of the molecule adsorbed on the K terminated double layer kink.

group binding to the K kink termination and the other two groups binding to adjacent sites coordinated by two K ions on the inner step edge. The lowest energy structure of the truxene molecule adsorbed on the Br terminated double atomic kink is shown in Figure 9a, which corresponds to a binding energy of 1.33 eV. This structure is characterized by one CN group binding to the deep potential well formed by the three K ions in the kink corner and the other two groups bound to adjacent two coordinated K sites on the inner step edge. The chirality of the truxene molecule does not significantly affect the adsorption energy in this case.

Molecular dynamics simulations of these conformations at room temperature fail to observe any full molecular transitions away from the kink in either case over long simulation times (approximately 100 ns). In each case, the difference in the potential energy surface from that on the perfect (010) step edge is due to the one CN binding group that is bound to either the K termination or the triple K coordinated corner site, and so it is these sites which are critical to the long residence time of the molecule.

## CONCLUSION

We have shown that truxene molecules functionalized with cyanobenzyl groups can be deposited at the nanoscale patterned KBr(001) surface at RT and imaged with the NC-AFM. This confirms the underlying design concept used in when choosing the adsorbate—using a flexible molecule functionalized with several long polar binding groups. The surprising result of this study is that, in spite of a relatively strong binding to the surface, the molecule is very mobile on a terrace. Another design concept specific to this study concerns patterning of the surface with monolayer step edges and kinks. This allowed us to observe three different regimes of molecular diffusion in the images obtained with the NC-AFM. The experimental images apparently show a hierarchy of surface molecular mobility: the molecules diffuse too rapidly on the perfect surface to be observed and are immobilized over the time scale of the experiment at kink sites. Straight monolayer step edges act as tracks for one-dimensional diffusion of molecules, which is observed directly in these images. Here, the residence times can be measured by analyzing fuzzy patterns in the images. This direct and simultaneous observation of several different regimes of molecular motion offers a powerful insight into processes occurring on a surface at room temperature.

The modeling of the molecular adsorption and diffusion replicates the three regimes of motion observed experimentally and elucidates the underlying processes driving the different types of molecular motion. First, that the interaction of the molecule with the surface is

mostly limited to the anchoring groups, while the truxene core of the molecule is separated from and interacts weakly with the surface. The modeling also shows that the combination of all three binding groups interacting independently with different surface binding sites is critical to the anchoring of the molecule as a whole and the dynamical behavior observed. A single cyano group is insufficient to bind the molecule to the surface or step edge and to immobilize the molecule at kink sites—a conclusion which is supported by the failure of single isolated molecules with only one cyano group to be observed on this surface. The structure of the molecule is also important; the flexibility of the individual groups to allow them to bind to specific sites proved critical for the anchoring of the molecules.

The rate of diffusion of the molecule on the surface and along the step edge and the binding to the step edge and kinks are results of the combined motion of all three binding groups. The resultant thermally driven motion of the molecule is complex and depends on how the binding groups are attached to the molecular backbone and how freely they are able to move. The large differences in the mobility of the molecule on the terrace and the monolayer step edge and kinks are due to not only the increase in the absolute binding of the individual binding groups in the deep potential wells formed by adjacent K atoms in the step and kinks but also the confinement of the molecular structure at these sites and the corresponding loss of entropy in the systems.

Realistic modeling of the type performed in this study provides a remarkable level of detail of the mechanism of adsorption and diffusion of the molecule on each type of surface feature. Quantitatively, the rates of diffusion are significantly different than those observed experimentally, which is most likely due to the fact that the model employed is underestimating the magnitude of the absolute binding to the surface, which will not affect the overall mechanisms of motion. Additionally, the tip of the NC-AFM can interact with the surface and adsorbates strongly at very close approach to the surface, which may significantly alter the potential energy surface for diffusive processes—in fact, there is evidence for this in Figure 4, where the asymmetric stripes are observed.

To summarize, using the design criteria based on previous experimental studies and theoretical modeling, we conceived, deposited, and studied a functionalized hydrocarbon molecule on an inert insulating surface. This study shows how the combination of NC-AFM experiments and theoretical modeling can help to provide an unprecedented insight into the processes of surface diffusion, even of relatively complex systems.

## METHODS

**Surface Preparation.** The KBr crystals were cleaved in air and subsequently inserted into the vacuum system with a base pres-

sure better than  $1 \times 10^{-10}$  mbar. The cleavage of a single KBr crystal exposes the (001) plane, where large terraces (of up to 1  $\mu\text{m}$ ) are separated by monatomic steps or more rarely by multi-

layer steps. The crystals were then annealed at 393 K in order to remove water and possible charges from their surfaces. This procedure provides clean surfaces, where steps are often curved due to the interaction with water. Afterward, the crystal was annealed at 413 K and irradiated with a small dose of 1 keV electrons. The molecules were evaporated from an effusion cell kept at 438 K onto the KBr(001) surface, kept at 428 K for 5 min, which resulted in the coverage of approximately 40% of a monolayer.

**Experimental Imaging.** A home-built NC-AFM microscope<sup>46</sup> was used to characterize the surface and molecular adsorbates. Silicon cantilevers (Nanosensors NCL,  $k = 42 \text{ N/m}$ ,  $Q = 21\,000$ ) were employed and oscillated with a typical amplitude of 20 nm peak-to-peak. Images were analyzed using WSxM software.<sup>64</sup>

**Ab Initio Calculations.** These calculations were performed using the GUESS embedded cluster code<sup>50</sup> which employs the GAUSSIAN98 package.<sup>52</sup> In these calculations, the surface is represented by a stoichiometric cluster of KBr ( $\text{K}_{16}\text{Br}_{16}$ ) surrounded by effective core potential atoms and is embedded in a region of shell model ions which are free to relax. The cluster is further embedded in an array of point charges to reproduce the Madelung potential of the crystal. The atoms in the surface cluster are treated with lanl2dz basis functions (modified to reproduce the ionization potential and electron affinity of K and Br, respectively) and lanl2 core pseudo-potentials.<sup>52</sup> The atoms of the molecules are treated using 6-31G(d) basis functions. Basis set superposition errors are estimated using the counterpoise method.<sup>53</sup> These calculations employed the B3LYP hybrid functional.<sup>54,55</sup>

**Interatomic Potentials.** The molecule surface force field employs Buckingham potentials and RESP atomic charges (as used in ref 58). The details of the fitting procedure, the fitted parameters of the Buckingham potentials, and the list of atomic charges are included as Supporting Information. These potentials were then combined with intramolecular potentials for the truxene molecule from Cornell *et al.*<sup>58</sup> with additional potentials for the nitrile groups<sup>59</sup> and potentials for the KBr surface from Catlow *et al.*<sup>60</sup> The classical energy and molecular dynamics calculations in this study are performed with the SciFi atomistic simulation code<sup>61</sup> and the DLPoly molecular dynamics code.<sup>62</sup>

**Acknowledgment.** We acknowledge financial support from the European Project IST-FET Pico-Inside. Additionally, the Basel group acknowledges support from Swiss National Science Foundation, the Swiss National Center of Competence in Research on Nanoscale Science, and the ESF-EUROCORE program FANAS. The Tarragona group acknowledges support from MEC (CTQ2007-60745/BQU and Consolider Ingenio 2010, Grant CSD2006-0003). We are grateful to M. L. Sushko and A. S. Foster for useful discussions.

**Supporting Information Available:** Details of the force-field parameter fitting procedure, along with the parameters and RESP charges. An animation of the real-time evolution of the structure of the molecule adsorbed on the KBr(001) surface over a period of 500 ps from a side view is presented, in addition to a top view animation of the diffusion over a period of 1 ns. A side view animation of the evolution of the structure of the molecule bound to a step edge over 5 ns is also presented. Complete ref 52. This material is available free of charge via the Internet at <http://pubs.acs.org>.

## REFERENCES AND NOTES

- Aviram, A.; Ratner, M. Progress in Molecular Scale Devices and Circuits. *Chem. Phys. Lett.* **1974**, *29*, 277–283.
- Joachim, C.; Gimzewski, J.; Schlittler, R. R.; Chavy, C. Electronic Transparency of a Single  $C_{60}$  Molecule. *Phys. Rev. Lett.* **1995**, *74*, 2102–2105.
- Joachim, C.; Gimzewski, J.; Aviram, A. Flexible Electronic Futures. *Nature* **2000**, *408*, 541–548.
- Joachim, C. Bonding More Atoms Together for a Single Molecule Computer. *Nanotechnology* **2002**, *13*, R1.
- Heath, J. R.; Ratner, M. A. Molecular Electronics. *Phys. Today May* **2003**, *43*.
- Eigler, D. M.; Schweizer, E. K. Positioning Single Atoms with a Scanning Tunnelling Microscope. *Nature* **1990**, *344*, 524–526.
- Crommie, M. F.; Lutz, C. P.; Eigler, D. M. Confinement of Electrons to Quantum Corrals on a Metal Surface. *Science* **1993**, *262*, 218–220.
- Heinrich, A. J.; Lutz, C. P.; Gupta, J. A.; Eigler, D. M. Molecule Cascades. *Science* **2002**, *298*, 1381–1387.
- Sugimoto, Y.; Abe, M.; Hirayama, S.; Oyabu, N.; Custance, O.; Morita, S. Atom Inlays Performed at Room Temperature Using Atomic Force Microscopy. *Nat. Mater.* **2005**, *4*, 156–159.
- Ternes, M.; Lutz, C. P.; Hirjibehedin, C. F.; Giessibl, F. J.; Heinrich, A. J. The Force Needed To Move an Atom on a Surface. *Science* **2008**, *319*, 1066–1069.
- Gourdon, A. Synthesis of “Molecular Landers”. *Eur. J. Org. Chem.* **1998**, 2797–2801.
- Nilius, N.; Wallis, T. M.; Ho, W. Development of One-Dimensional Band Structure in Artificial Gold Chains. *Science* **2002**, *297*, 1853–1856.
- Miwa, J. A.; Weigelt, S.; Gersen, H.; Besenbacher, F.; Rosei, F.; Linderoth, T. R. Azobenzene on Cu(110): Adsorption Site-Dependent Diffusion. *J. Am. Chem. Soc.* **2006**, *128*, 3164–3165.
- Weigelt, S.; Busse, C.; Petersen, L.; Rauls, E.; Hammer, B.; Gothelf, K. V.; Besenbacher, F.; Linderoth, T. R. Chiral Switching by Spontaneous Conformational Change in Adsorbed Organic Molecules. *Nat. Mater.* **2006**, *5*, 112–117.
- Alemani, M.; Peters, M. V.; Hecht, S.; Rieder, K. H.; Moresco, F.; Grill, L. Electric Field-Induced Isomerization of Azobenzene by STM. *J. Am. Chem. Soc.* **2006**, *128*, 14446–14447.
- Iancu, V.; Hla, S. W. Realization of a Four-Step Molecular Switch in Scanning Tunneling Microscope Manipulation of Single Chlorophyll-a Molecules. *Proc. Natl. Acad. Sci. U.S.A.* **2006**, *103*, 13718–13721.
- Perepichka, D. F.; Bryce, M. R.; Pearson, C.; Petty, M. C.; McInnes, E. J. L.; Zhao, J. P. A Tetraphiafulvalene-tetracyanoquinodimethane Diad: Extremely Low HOMO–LUMO Gap, Redox and Spectroscopic Properties, and Formation of Langmuir Blodgett Films. *Angew. Chem., Int. Ed.* **2003**, *42*, 4635–4638.
- Perepichka, D. F.; Bryce, M. R. Molecules with Exceptionally Small HOMO–LUMO Gaps. *Angew. Chem., Int. Ed.* **2005**, *44*, 5370–5373.
- Bendikov, M.; Wudl, F.; Perepichka, D. F. Molecular Materials Across Fields: TTFs, Fullerenes and Acenes. *Chem. Rev.* **2004**, *104*, 4891–4946.
- Oleynik, I. I.; Kozhushnina, M. A.; Posvyanskii, V. S.; Yu, L. Rectification Mechanism in Diblock Oligomer Molecular Diodes. *Phys. Rev. Lett.* **2006**, *96*, 096803–096807.
- Barth, J. V.; Weckesser, J.; Cai, C.; Günter, P.; Bürgi, L.; Jeandupeux, O.; Kern, K. Building Supramolecular Nanostructures at Surfaces by Hydrogen Bonding. *Angew. Chem., Int. Ed.* **2000**, *39*, 1230–1234.
- Hecht, S. Welding, Organizing, and Planting Molecules on Substrate Surfaces—Promising New Approaches towards Nanoarchitectonics from the Bottom up. *Angew. Chem., Int. Ed.* **2003**, *42*, 24–26.
- Theobald, J. A.; Oxtoby, N. S.; Phillips, M. A.; Champness, N. R.; Beton, P. H. Controlling Molecular Deposition and Layer Structure with Supramolecular Surface Assemblies. *Nature* **2003**, *424*, 1029–1031.
- Rosei, F.; Schunack, M.; Jiang, P.; Gourdon, A.; Lægsgaard, E.; Stensgaard, I.; Joachim, C.; Besenbacher, F. Organic Molecules Acting as Templates on Metal Surfaces. *Science* **2002**, *296*, 328–331.
- Maier, S.; Fendt, L.; Zimmerli, L.; Glatzel, Th.; Pfeiffer, O.; Diederich, F.; Meyer, E. Nanoscale Engineering of Molecular Porphyrin Wires on Insulating Surfaces. *Small* **2008**, *4*, 1115–1118.
- Zimmerli, L.; Maier, S.; Glatzel, Th.; Gnecco, E.; Pfeiffer, O.; Diederich, F.; Fendt, L.; Meyer, E. Formation of Molecular Wires on Nanostructured KBr. *J. Phys. Conf. Ser.* **2007**, *61*, 1357–1360.

27. Sushko, M. L.; Gal, A. Y.; Shluger, A. L. Probing Organic Layers on the TiO<sub>2</sub>(110) Surface. *J. Phys. Chem. B* **2006**, *110*, 4853–4862.
28. Trevethan, T.; Shluger, A. L. Modeling the Diffusive Motion of Large Organic Molecules on Insulating Surfaces. *J. Phys. Chem. C* **2008**, *112*, 19577–19583.
29. Bennewitz, R.; Pfeiffer, O.; Schar, S.; Barwick, V.; Meyer, E.; Kantorovich, L. N. Atomic Corrugation in NC-AFM of Alkali Halides. *Appl. Surf. Sci.* **2002**, *188*, 232–237.
30. Such, B.; Czuba, P.; Piatkowski, P.; Szymonski, M. AFM Studies of Electron-Stimulated Desorption Process of KBr(001) Surface. *Surf. Sci.* **2000**, *451*, 203–207.
31. Morita, S.; Wiessendanger, R.; Meyer, E., Eds. *Non-Contact Atomic Force Microscopy*; Springer: Berlin, 2002; 450 pp.
32. Giessibl, F. Advances in Atomic Force Microscopy. *Rev. Mod. Phys.* **2003**, *75*, 949–983.
33. Garcia, R.; Perez, R. Dynamic Atomic Force Microscopy Methods. *Surf. Sci. Rep.* **2002**, *47*, 197–301.
34. Schlettwein, D.; Back, A.; Schilling, B.; Fritz, T.; Armstrong, N. R. Ultrathin Films of Perylenedianhydride and Perylenebis(dicarboximide) Dyes on (001) Alkali Halide Surfaces. *Chem. Mater.* **1998**, *10*, 601–612.
35. Nony, L.; Bennewitz, R.; Pfeiffer, O.; Gnecco, E.; Baratoff, A.; Meyer, E.; Eguchi, T.; Gourdon, A.; Joachim, C. Cu-TBPP and PTCDA Molecules on Insulating Surfaces Studied by Ultra-High-Vacuum Non-Contact AFM. *Nanotechnology* **2004**, *15*, S91.
36. Proehl, H.; Nitsche, R.; Dienel, T.; Leo, K.; Fritz, T. *In Situ* Differential Reflectance Spectroscopy of Thin Crystalline Films of PTCDA on Different Substrates. *Phys. Rev. B* **2005**, *71*, 165207–165221.
37. Proehl, H.; Dienel, T.; Nitsche, R.; Fritz, T. Formation of Solid-State Excitons in Ultrathin Crystalline Films of PTCDA: From Single Molecules to Molecular Stacks. *Phys. Rev. Lett.* **2004**, *93*, 097403–097407.
38. Kunstrmann, T.; Schlarb, A.; Fendrich, M.; Wagner, Th.; Möller, R.; Hoffmann, R. Dynamic Force Microscopy Study of 3,4,9,10-Perylenetetracarboxylic Dianhydride on KBr(001). *Phys. Rev. B* **2005**, *71*, 121403–121407.
39. Dienel, T.; Loppacher, C.; Mannsfeld, S. C. B.; Forker, R.; Fritz, T. Growth-Mode-Induced Narrowing of Optical Spectra of an Organic Adlayer. *Adv. Mater.* **2008**, *20*, 959–963.
40. Schütte, J.; Bechstein, R.; Rahe, P.; Rohlfing, M.; Kühnle, A.; Langhals, H. Imaging Perylene Derivatives on Rutile TiO<sub>2</sub>(110) by Noncontact Atomic Force Microscopy. *Phys. Rev. B* **2009**, *80*, 045428–045436.
41. Ferron, J.; Miranda, R.; de Miguel, J. J. Atomic Jumps during Surface Diffusion. *Phys. Rev. B* **2009**, *79*, 245407–245416.
42. Park, J. H.; Aluru, N. R. Surface Diffusion of *n*-Alkanes: Mechanism and Anomalous Behavior. *Chem. Phys. Lett.* **2007**, *447*, 310–315.
43. Otero, R.; Hummelink, F.; Sato, F.; Legoa, S. B.; Thostrup, P.; Lægsgaard, E.; Stensgaard, I.; Galvão, D. S.; Besenbacher, F. Lock-and-Key Effect in the Surface Diffusion of Large Organic Molecules Probed by STM. *Nat. Mater.* **2004**, *3*, 779–782.
44. de Frutos, O.; Granier, T.; Gomez-Lor, B.; Jimenez-Barbero, J.; Monge, A.; Gutierrez-Puebla, E.; Echavarren, A. M. Synthesis and Self-Association of *syn*-5,10,15-Trialkylated Truxenes. *Chem.—Eur. J.* **2002**, *8*, 2879–2890.
45. Wohlfart, K.; Schnell, M.; Grabow, J.-W.; Küpper, J. Precise Dipole Moment and Quadrupole Coupling Constants of Benzonitrile. *J. Mol. Spectrosc.* **2008**, *247*, 119–121.
46. Howald, L.; Meyer, E.; Lüthi, R.; Haefke, H.; Overney, R.; Rudin, H.; Güntherodt, H.-J. Multifunctional Probe Microscope for Facile Operation in Ultrahigh Vacuum. *Appl. Phys. Lett.* **1993**, *63*, 117–119.
47. Hofer, W. A.; Foster, A. S.; Shluger, A. L. Theories of Scanning Probe Microscopes at the Atomic Scale. *Rev. Mod. Phys.* **2003**, *75*, 1287–1331.
48. Rost, M. J.; Frenken, J. M. W. Comment on: Real Space Investigation of the Roughening and Deconstruction Transitions of Au(110). *Phys. Rev. Lett.* **2001**, *87*, 039603.
49. Watkins, M.; Trevethan, T.; Shluger, A. L.; Kantorovich, L. N. Dynamical Processes at Oxide Surfaces Studied with the Virtual Atomic Force Microscope. *Phys. Rev. B* **2007**, *76*, 245421–245428.
50. Sushko, P. V.; Shluger, A. L.; Catlow, C. R. A. Relative Energies of Surface and Defect States: *Ab Initio* Calculations of the MgO(001) Surface. *Surf. Sci.* **2000**, *450*, 153–170.
51. Hess, W. P.; Joly, A. G.; Gerrity, D. P.; Beck, K. M.; Sushko, P. V.; Shluger, A. L. Selective Laser Desorption of Ionic Surfaces: Resonant Surface Excitation of KBr. *J. Chem. Phys.* **2001**, *115*, 9463–9472.
52. Frisch, M. J. et al. *Gaussian 98*; Gaussian, Inc.: Wallingford, CT, 2004.
53. Boys, S. F.; Bernardi, F. The Calculation of Small Molecular Interactions by the Differences of Separate Total Energies. Some Procedures with Reduced Errors. *Mol. Phys.* **1970**, *19*, 553–566.
54. Becke, A. D. Density-Functional Thermochemistry. III. The Role of Exact Exchange. *J. Chem. Phys.* **1993**, *98*, 5648–5652.
55. Lee, C.; Yang, W.; Parr, R. G. Development of the Colle-Salvetti Correlation-Energy Formula into a Functional of the Electron Density. *Phys. Rev. B* **1988**, *37*, 785–789.
56. Head-Gordon, M.; Pople, J. A.; Frisch, M. J. MP2 Energy Evaluation by Direct Methods. *Chem. Phys. Lett.* **1988**, *153*, 503–506.
57. Watkins, M.; Trevethan, T.; Sushko, M. L.; Shluger, A. L. Designing Molecular Architecture to Control Diffusion and Adsorption on Insulating Surfaces. *J. Phys. Chem. C* **2008**, *112*, 4226–4231.
58. Cornell, W. D.; Cieplak, P.; Bayly, C. I.; Gould, I. R.; Mertz, K. M.; Ferguson, D. M.; Spellmeyer, D. C.; Fox, T.; Caldwell, J. W.; Kollman, P. A. A Second Generation Force Field for the Simulation of Proteins, Nucleic Acids, and Organic Molecules. *J. Am. Chem. Soc.* **1995**, *117*, 5179–5197.
59. Howard, A. E.; Cieplak, P.; Kollman, P. A. A Molecular Mechanical Model That Reproduces the Relative Energies for Chair and Twist-Boat Conformations of 1,3-Dioxanes. *J. Comput. Chem.* **1995**, *16*, 243–261.
60. Catlow, C. R. A.; Diller, K. M.; Norgett, M. J. Interionic Potentials for Alkali Halides. *J. Phys. C* **1977**, *10*, 1395–1412.
61. Kantorovich, L.; Trevethan, T.; Foster, A. S. Self-Consistent Image Force Interaction Code (<http://www.cmmmp.ucl.ac.uk/~lev/codes/SciFi/manual-3-51/index.html>).
62. Smith, W.; Forester, T. R. DL POLY2: A General Purpose Parallel Molecular Dynamics Simulation Package. *J. Mol. Graphics* **1996**, *14*, 136–141.
63. Kannan, S.; Zacharias, M. Simulated Annealing Coupled Replica Exchange Molecular Dynamics—An Efficient Conformational Sampling Method. *J. Struct. Biol.* **2009**, *166*, 288–294.
64. Horcas, I.; Fernandez, R.; Gomez-Rodriguez, J. M.; Colchero, J.; Gomez-Herrero, J.; Baro, A. M. WSXM: A Software for Scanning Probe Microscopy and a Tool for Nanotechnology. *Rev. Sci. Instrum.* **2008**, *79*, 013705–013713.